NAA-SR-4869
REACTORS-GENERAL
37 PAGES

VALVE STEM FREEZE SEAL FOR HIGH-TEMPERATURE SODIUM

By
J. S. McDONALD

ATOMICS INTERNATIONAL

A DIVISION OF NORTH AMERICAN AVIATION, INC.
P.O. BOX 309 CANOGA PARK, CALIFORNIA

CONTRACT: AT(11-1)-GEN-8
ISSUED: JUL 30 1960

DISTRIBUTION

This report has been distributed according to the category "Reactors-General" as given in "Standard Distribution Lists for Unclassified Scientific and Technical Reports" TID-4500 (15th Ed.), August 1, 1959. A total of 625 copies was printed.

CONTENTS

FIGURES

FIGURES

ABSTRACT

An experimental study of valve stem freeze seals was undertaken as part of the effort to develop components for high temperature service in advanced sodium-cooled reactor systems. An experimental model, which was suitable for use with a 6-in. size valve, operated satisfactorily under a variety of conditions. The freeze seal region was cooled by natural convection to ambient atmosphere; cooling by both circumferential and longitudinal finned sections was experimentally studied. The operating conditions included sodium bulk temperatures up to 1300°F, sodium pressures up to 75 psig, and ambient temperatures as high as 150°F. Anticonvection rings were positioned in the sodium-filled annulus between stem and stemguide, and the effects of their presence was studied.

Predictions of temperature profiles along the stem, using several different analytical methods, were compared with experimental results. Based on a comparison of predicted and actual results, it is considered that reliable valve freeze seals may be designed for high-temperature sodium systems.

I. INTRODUCTION

As the operating temperatures of sodium cooled reactors continue to increase, greater demands will be placed on coolant system components. An important problem, in the field of sodium technology, has been the development of a seal for valves to prevent the leakage of sodium through the stem-stem guide annulus. Packing-type seals used in the conventional manner have been unsatisfactory for sodium service at high temperatures.[1] The use of bellows seals is expensive and presents reliability questions for which satisfactory answers do not exist. A development program at Oak Ridge National Laboratory (ORNL) established the feasibility of obtaining a satisfactory seal by freezing sodium in the annulus around the stem.[2] However, freeze seals have not in the past been used successfully at system pressures above about 50 psig, because higher pressures cause the sodium to extrude through the annulus and out of the seal region.[3] Thus, Atomics International undertook the development of valve stem freeze seals to meet the high temperature needs of advanced sodium cooled reactor systems. In addition, it was desired to provide a greater margin of safety with respect to the ability of the freeze seal to withstand system pressure. To eliminate the need for a freeze seal auxiliary cooling system, the freeze section of the experimental model incorporated a finned surface which was cooled by free convection to the ambient atmosphere.

The chief objective in this effort was the development of a freeze seal which, with maximum sodium bulk temperatures of 1300°F, would perform the following functions:

a) Prevent the extrusion of sodium through the seal when system pressures are up to about 75 psig.

b) Prevent the entry of gas into the system when system pressures are low. (The seal is fitted with an inert gas backup chamber.)

c) Prevent the buildup of oxides in the stem-stem guide annulus over long-term operation. (This process comes about because the freeze seal acts as a diffusion cold trap; the oxide in turn acts as a cement, hindering movement of the valve stem.)

As part of the experimental effort it was desired to compare test results with the analytical predictions for both longitudinal and circumferential fins. In addition, it was intended to determine the optimum gas backup pressure and the oxide effects on the torque required to turn the stem.

II. METHOD USED AND DESCRIPTION OF EQUIPMENT

A. DESIGN OF UNIT

The experimental freeze seal was designed to be suitable for use with a 6-in. valve for sodium at maximum conditions of 1150°F and 75 psig for long-term operation, and 1300°F and 75 psig for short-term operation. Key dimensions of the experimental freeze seal section appear in Figure 1. Anticonvection

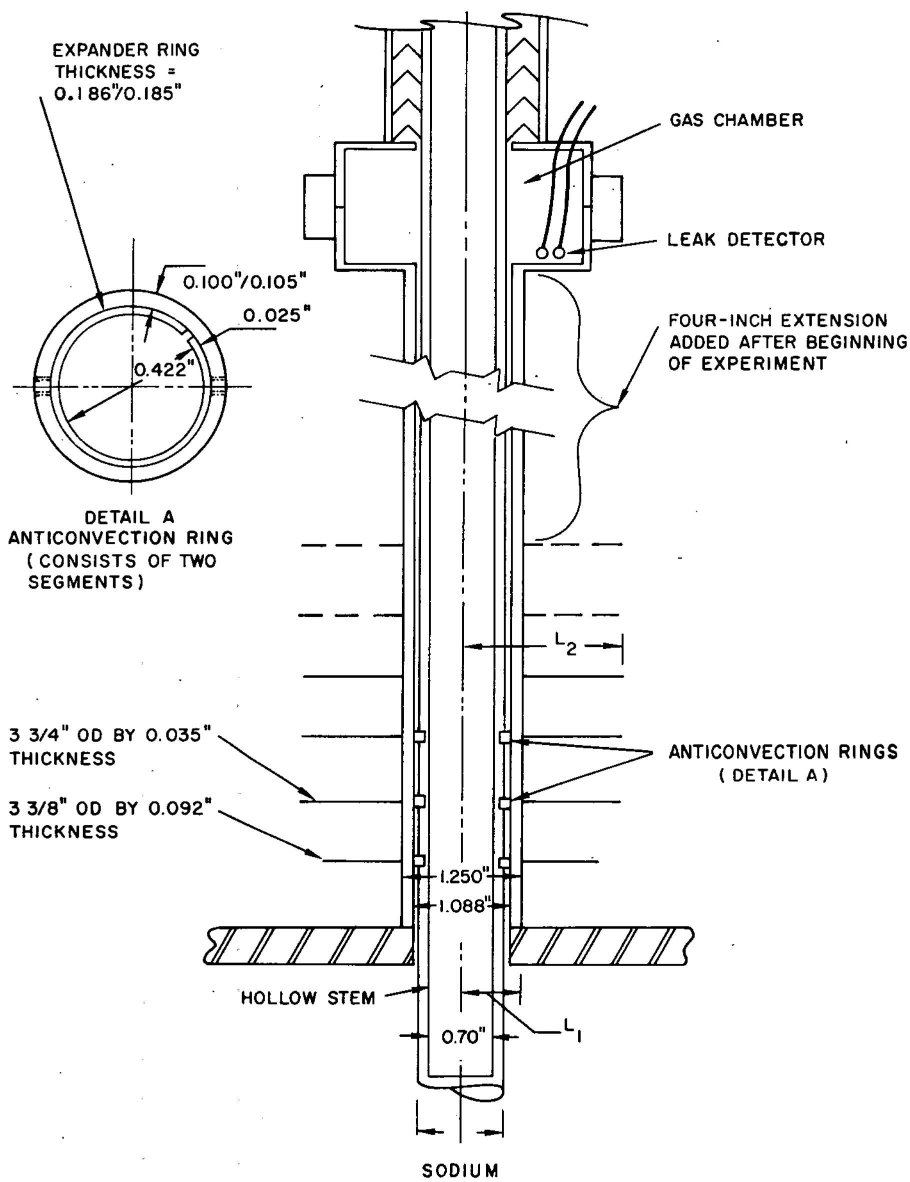

Figure 1. Freeze Seal Details

rings were positioned in the annulus between the vertical hollow stem and the stem guide to inhibit thermal convection of molten sodium. Fins were attached to the outer periphery of the stem guide. Located at the top of the freeze seal region was a chamber containing inert gas. Two different fin arrangements were used for free convection cooling to the surrounding atmosphere. The first consisted of circumferential fins (Figure 1), the second consisted of eight rectangular longitudinal fins located in radial planes about the stem guide periphery (Figure 2). The circumferential fins were spaced one inch apart vertically. It

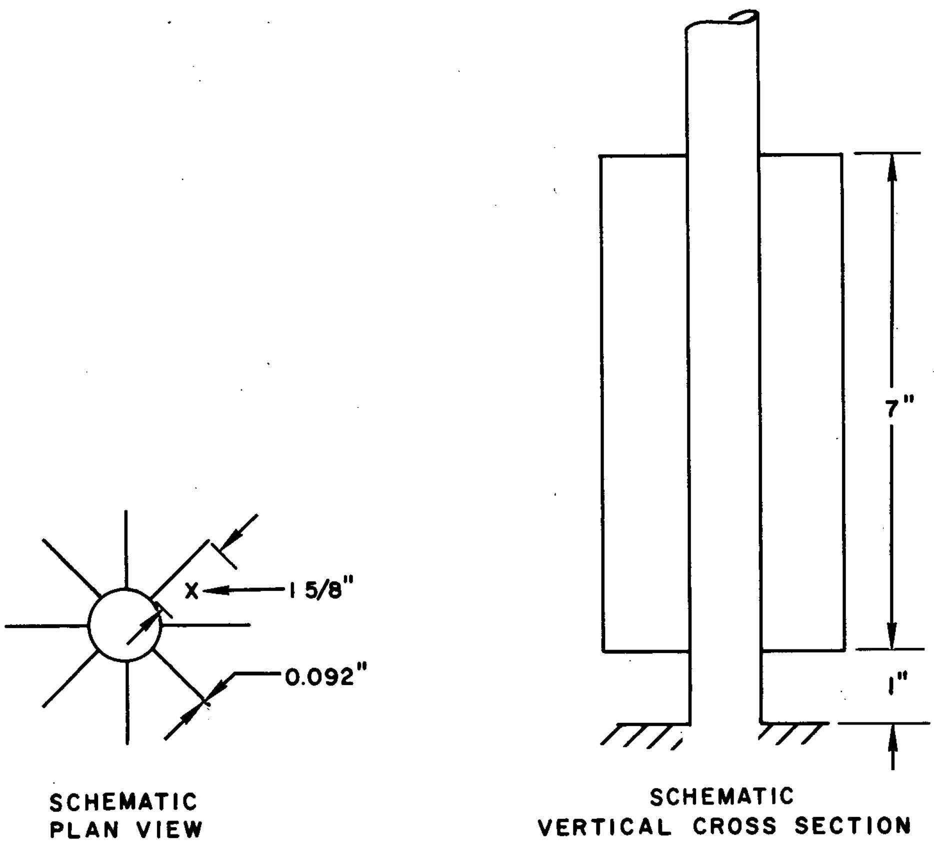

Figure 2. Longitudinal Fin Cooling Section

was recognized that the circumferential fin arrangement was not likely to be the most efficient design because of interference of the fins with the air flow pattern; however, this arrangement accommodated studies of energy transport up the stem-stem guide annulus by sodium natural convection. These studies are discussed in detail in a later section.

Three anticonvection rings were positioned in notches in the stem in the locations shown in Figure 1. A large scale detail of a ring is also shown in the figure. The rings used were a standard manufactured item*, fitted with backing springs which pressed the outer peripheries of the rings against the inside surface of the stem guide. Cast iron rings were purchased and plated with a one mil thickness of chromium. The rings were intended to perform three functions:

1) Reduce the heat transfer up the annulus.

2) Act as a barrier to sodium oxide diffusion into the seal region.

3) Increase the ability of the seal to withstand large top-to-bottom pressure differences.

The stem was designed specifically for rotary operation, although the design permits translational motion as well. A chamber, which was added at the top of the stem guide, permitted the pressure of the inert backup gas to be set as desired. The joint between the stem and the top of the chamber was sealed with Teflon chevron packing.

B. APPARATUS AND EXPERIMENTAL PROCEDURE

Pictured schematically in Figure 3 is the apparatus used in this experiment. The valve stem terminates in a dummy plug which rests on a seat in a 6-in. diameter by 2-ft long sodium pot. Projecting from the bottom of the pot is a small diffusion cold finger and a one-inch diameter line which connects the pot to a sodium expansion tank. The pressure of the cover gas in the expansion tank determines the bulk sodium pressure. A spark-plug type leak detector was located in the backup gas chamber to sense any extrusion of sodium from the seal. An AN-fitting was installed in the body of the gas chamber to facilitate clean-up operations in the event of sodium leakage.

The independent variables which were controlled during the experiment were sodium pressure and temperature, ambient temperature (in some cases), gas backup pressure, and the number of stem rotations. With the circumferential fin cooling section design, runs were made with four, five, and six fins in place; therefore, in a sense, the number of fins was an independent variable.

---

*Those used in this experiment were purchased from the Double Seal Ring Company, Fort Worth, Texas.

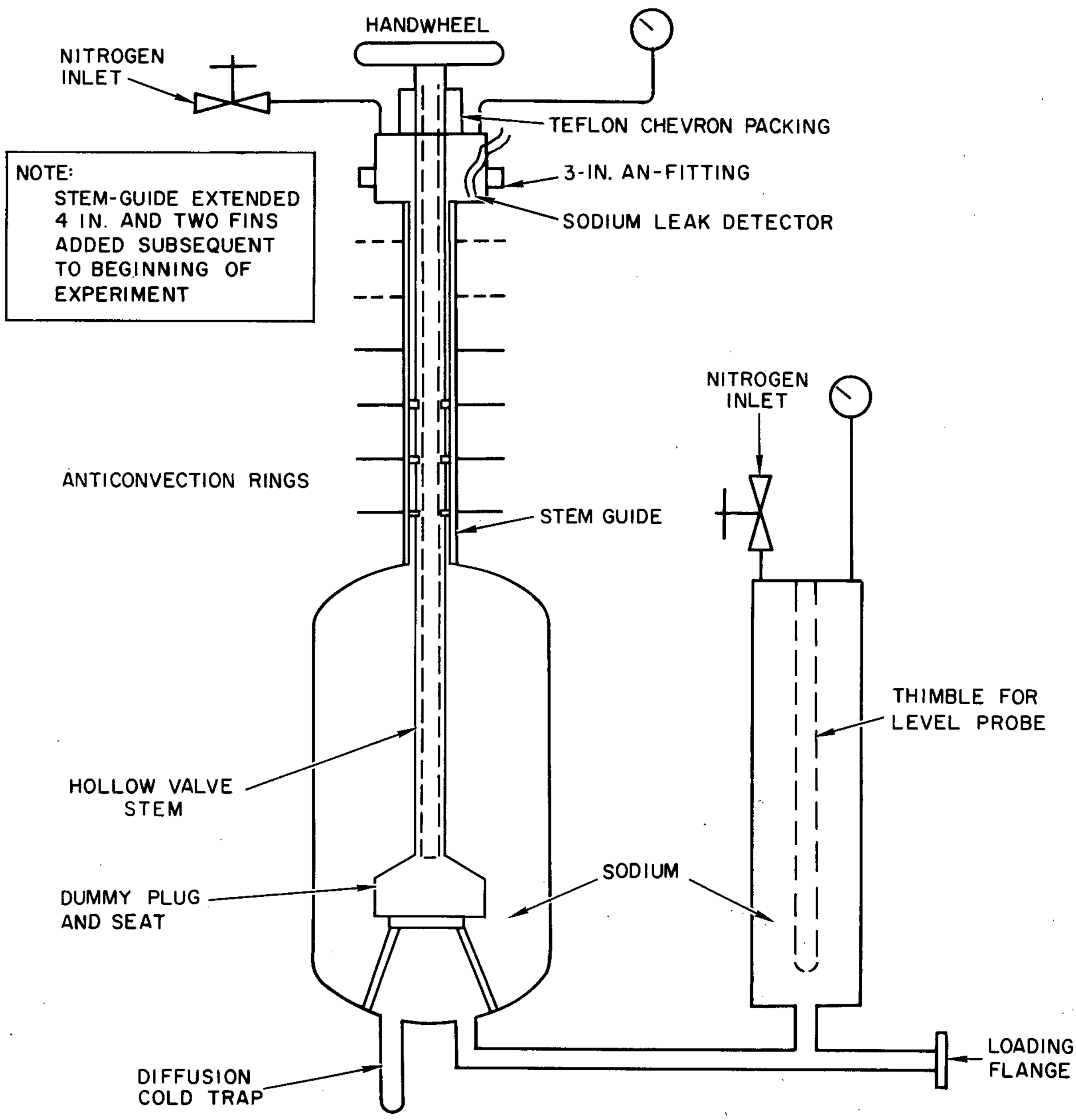

Figure 3. Apparatus for Stem Freeze Seal Experiment (circumferential fins in cooling section)

Measurements were made of temperatures in the sodium, in the ambient atmosphere, at the roots and tips of the fins, and at several locations on the stem guide. Also measured were the gas pressures and the torque required to rotate the stem.

Runs were first made with the circumferential fin cooling arrangement. Later, these fins were removed and the cooling section was fitted with longitudinal fins. The program was designed to determine as soon as possible the optimum gas backup pressure corresponding to a sodium pressure range of 0-75 psig. Early it became apparent that the gas backup pressure should not exceed one psig. When the backup pressure exceeded the sodium pressure by more than one psi, rotation of the stem was always accompanied by entry of gas down through the seal and into the sodium system.

As a second step in the program, cooling section temperature measurements were made at various sodium bulk temperatures between 600 and 1150°F for different values of sodium pressure between and including 0 and 75 psig. It was deduced from the analysis of data that a small volume of gas was trapped in the annulus below the bottom ring. This was confirmed by the observation of changes in sodium level in the expansion tank with changes in the sodium pressure. After many failures to expel the gas with the system hot, the rig was shut down (sodium was frozen) and a hole was drilled at the proper location under an inert gas blanket for the addition of a bleed line. Trapped gas was removed by a vacuum pump, and the small evacuation line was valved off. The sodium was melted, then allowed to fill the evacuation line and freeze. The line was then cut short and capped. Subsequent expansion tank sodium level measurement and heat transfer evidence verified that the trapped gas had been removed.

The freeze seal was then placed in operation with sodium at 1150°F and various pressures for 3 wk. During this time the valve stem was rotated an average of 10 times per day.

During the activities described above, the ambient temperature ranged from 76 to 100°F. Although it was thought that the freeze seal performance at higher ambient temperatures could be accurately predicted (based on the results obtained during the above runs), the experimental rig was modified to accommodate the simulation of a pipe gallery atmosphere. The test assembly was enclosed in an insulated sheet-metal box and an air heater was installed (in such a fashion as not to radiate directly onto the freeze seal section). Runs were then made with 150°F ambient temperatures. The sodium temperature was set at 1150 and 1300°F and was twice reduced to 600°F for a short length of time. The sodium pressure was cycled between 0 and 75 psig during the above runs.

Following the conclusion of runs with the circumferential fin cooling arrangement, the freeze seal section was dismantled and inspected, and a stem-guide sleeve fitted with longitudinal fins installed. The experimental operations with this second cooling arrangement were similar to those with the first, the maximum temperature and pressure attained having been 1300°F and 75 psig. After completion of these runs the unit was again dismantled and inspected.

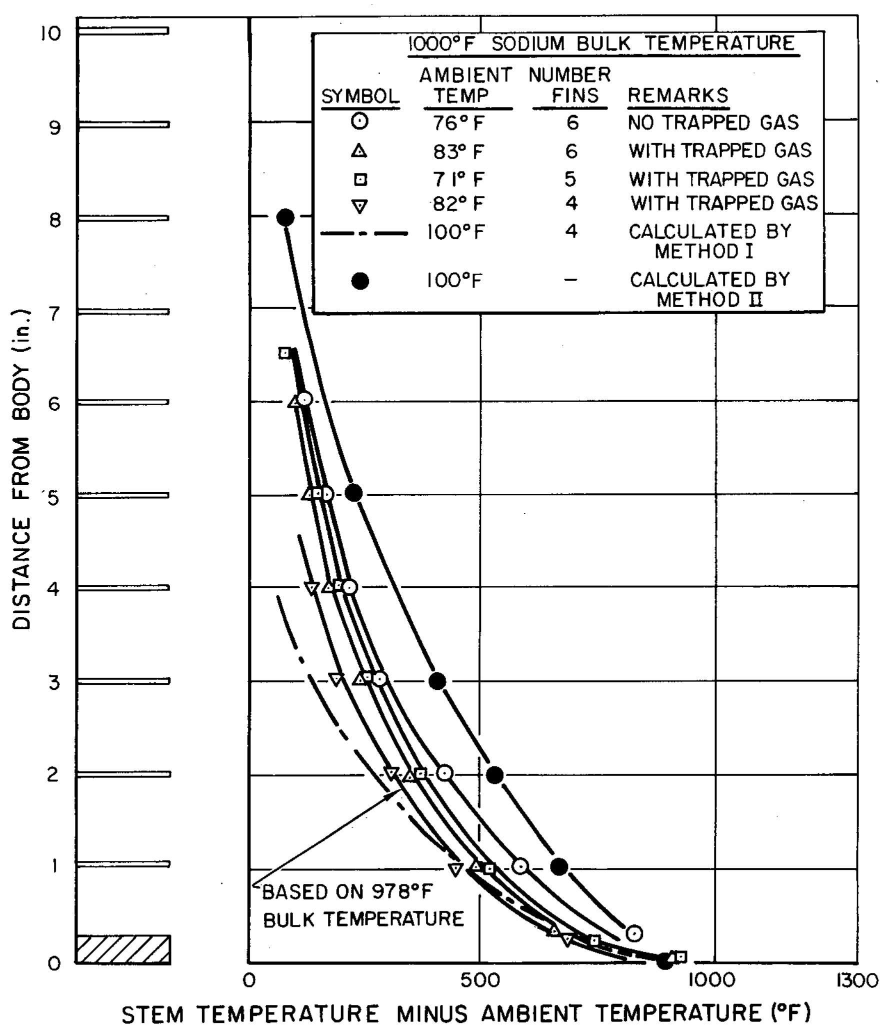

Figure 4. Temperature Profiles for T_O of 1000°F (circumferential fins)

III. DISCUSSION OF EXPERIMENTAL RESULTS AND ANALYSIS

A. GENERAL SUMMARY

The experimental unit performed satisfactorily using each of the cooling fin arrangements. With the circumferential fin design, the seal operated with sodium at 1150°F and at pressures ranging from 0-75 psig for a total of 500 hr. Ambient temperatures during this time varied from 79 to 150°F, and the stem was rotated a total of 800 times.

A total of 126 hr was logged with a sodium bulk temperature of 1300°F and pressures up to 75 psig. The ambient temperatures during this time were 100 and 150°F and the stem was rotated 15 times.

After the circumferential fins were replaced by longitudinal fins, the seal operated with the bulk sodium temperature at 1300°F for 150 hr and at 1150°F for 50 hr. The sodium pressure during this series was 75 psig during the working day and was reduced to one psig during the overnight periods. The stem was rotated 30 times, and the maximum ambient temperature attained while frozen sodium remained in the annulus (with bulk temperature of 1300°F) was 120°F. In one instance, the seal melted when the ambient temperature was permitted to rise too high.

It was determined that the gas backup pressure above the seal should not exceed one psig. Higher backup pressures caused blowing of gas through the seal when the sodium pressure was less than one psig. In addition to rotary motion, a one-inch amplitude translational motion was imparted to the stem for 10 cycles with the bulk sodium at 1150°F and60 psig. The seal held satisfactorily during this operation.

A subsequent section compares the experimental results with the results predicted by theoretical methods. In addition, there follows a discussion of the heat transport effects of natural convection up the annulus, and observations relative to the presence of sodium oxide in the seal region.

B. TEMPERATURE PROFILES

Figures 4, 5, 6, and 7 show vertical temperature profiles along the stem for various experimental conditions. Appearing to the left of the curves in each

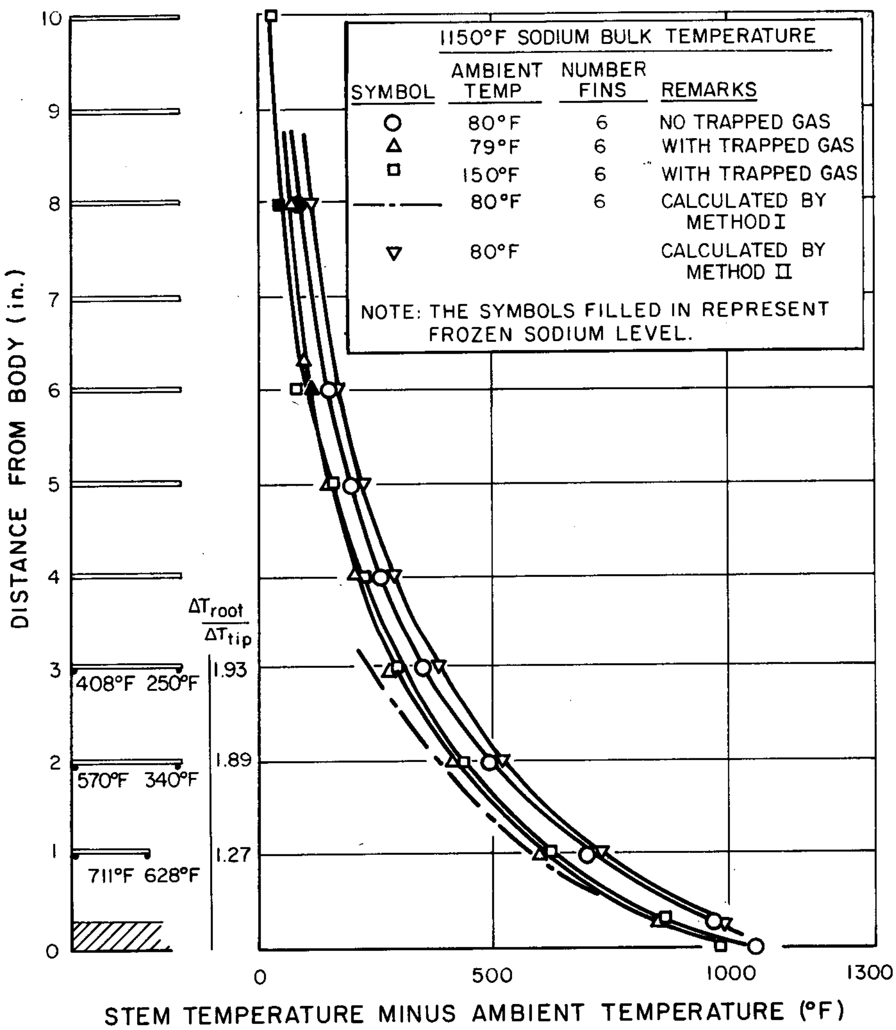

Figure 5. Temperature Profiles for T_o of 1150°F (circumferential fins)

figure is a representation of the freeze seal section physical profile, with vertical distances indicated. Such an illustration is included for each figure to clarify the correspondence between fin locations and temperature profile.

Figures 4, 5, and 6 pertain to the cooling arrangement which utilized circumferential fins. The curves in Figure 4 are for 1000°F sodium bulk temperature; similar curves are shown in Figure 5 for 1150°F sodium bulk temperature. Two curves appear in Figure 6, one for 620°F and the other for 1300°F sodium bulk temperature. The abscissa in each case is the difference between stem temperatures and the temperature of the ambient atmosphere since it is this potential difference that causes the heat flow. The close agreement between curves for similar sodium conditions, but different ambient conditions, points up the fact that the physical properties of air and the free convection pattern vary but little with temperature for the range in which we are interested. In Figure 4, the comparison of curves for the unit with four, five, and six fins indicates that the improvement in heat transfer diminishes rapidly as the number of fins is increased beyond four. This tends to confirm the conclusion reported in Reference 4 that almost equal heat transfer results are obtained (for a vertical finned stem) with three fins as with fifteen fins. A comparison may also be made with

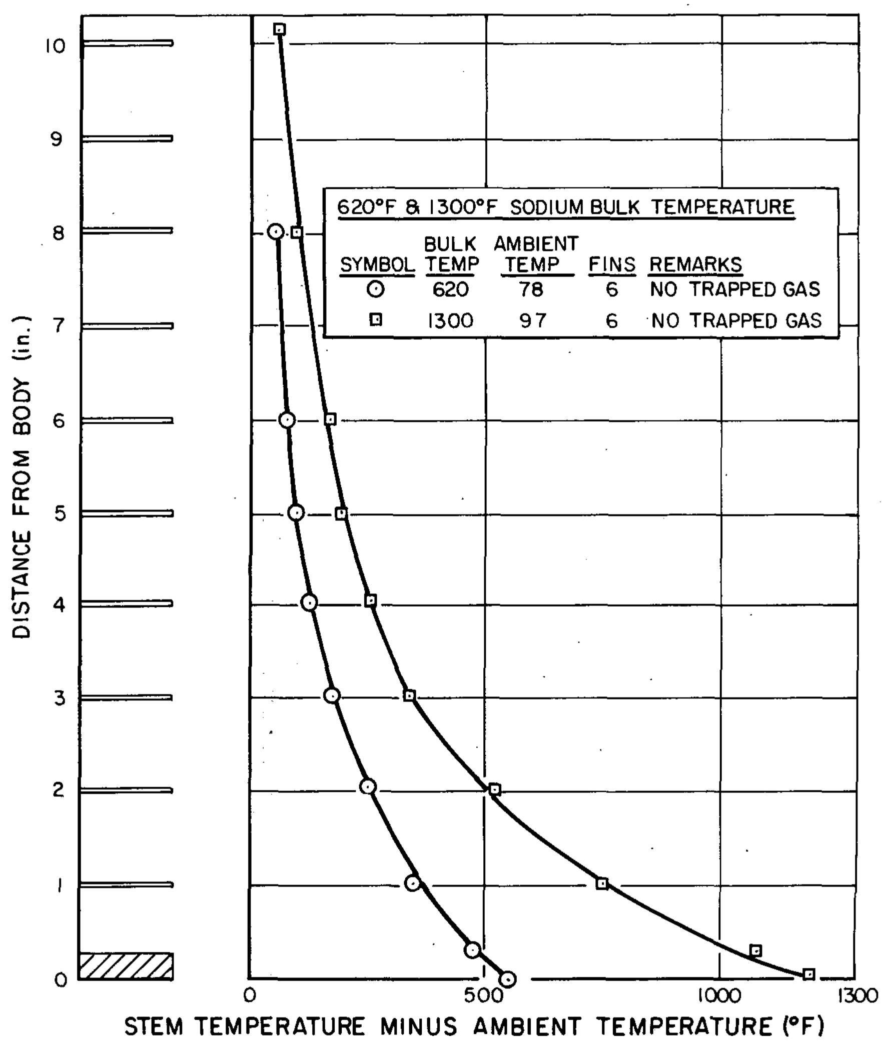

Figure 6. Temperature Profiles for T_o of 620°F, 1300°F (circumferential fins)

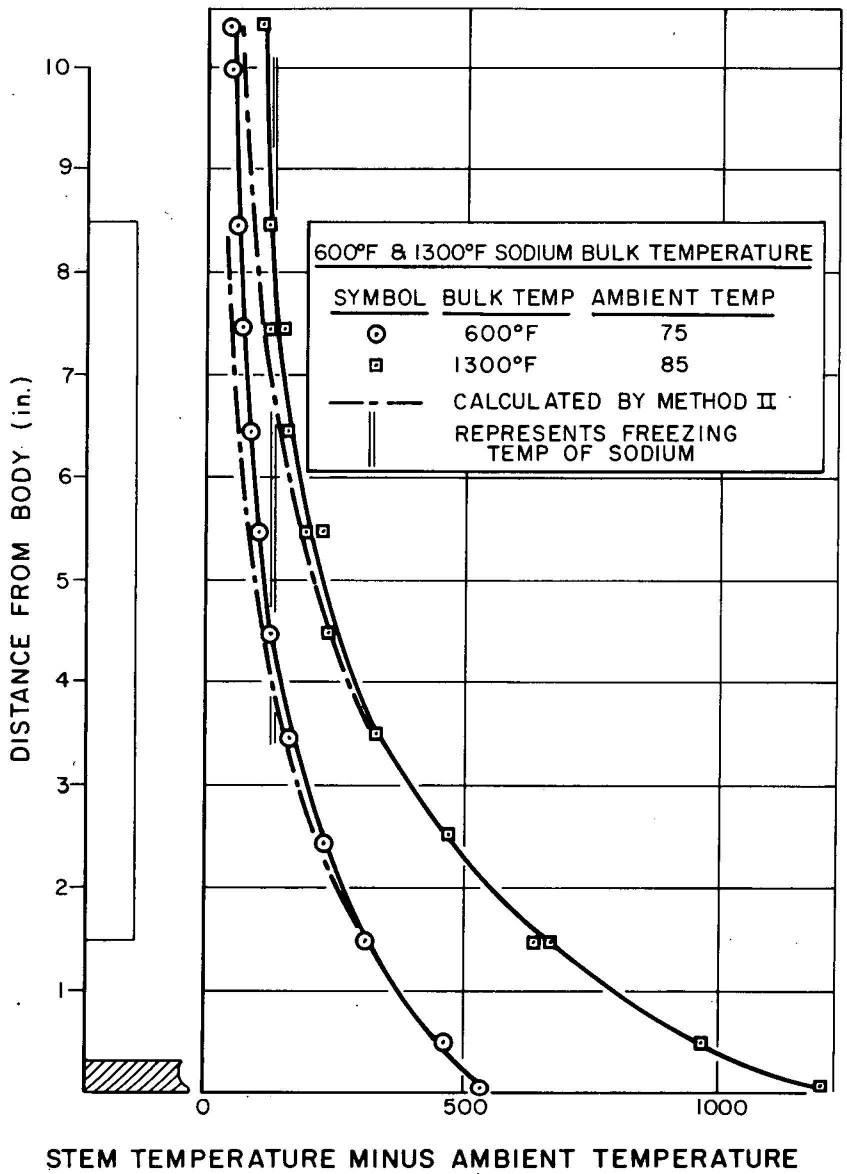

Figure 7. Temperature Profiles for T_o of 600°F, 1300°F (longitudinal fins)

the curves of the profiles with and without gas trapped below the bottom ring. It is seen that the gas reduced the heat transfer into the seal region. Also appearing in Figures 4 and 5 are curves calculated by Methods I and II discussed in the next section.

Figure 7, which is for the longitudinal fin design, illustrates the experimentally measured temperature profiles for sodium bulk temperatures of 600°F and 1300°F and curves calculated by Method II. The accuracy of predictions based on the analytical techniques will be discussed in the next section.

As a matter of interest, the cooling section profile of Figure 4 is marked with temperatures at the fin roots and tips, taken during a typical run. The "most favorable" fin design gives approximately a two-to-one ratio of fin to air temperature differences for the fin root and tip. Such ratios are also indicated in the figure, and it is noted that the designs were reasonably well optimized.

C. ANALYTICAL METHODS

1. Method I

This procedure consists of establishing a thermal network with lumped constants and, knowing the terminal temperatures (air and bulk sodium), finding the temperature distribution by an iterative method. This technique was used only in the case of the circumferential fin arrangement. An equivalent thermal circuit is represented in Figure 8. Also shown in Figure 8 is a schematic vertical cross section of the freeze seal indicating node point locations. It is implied

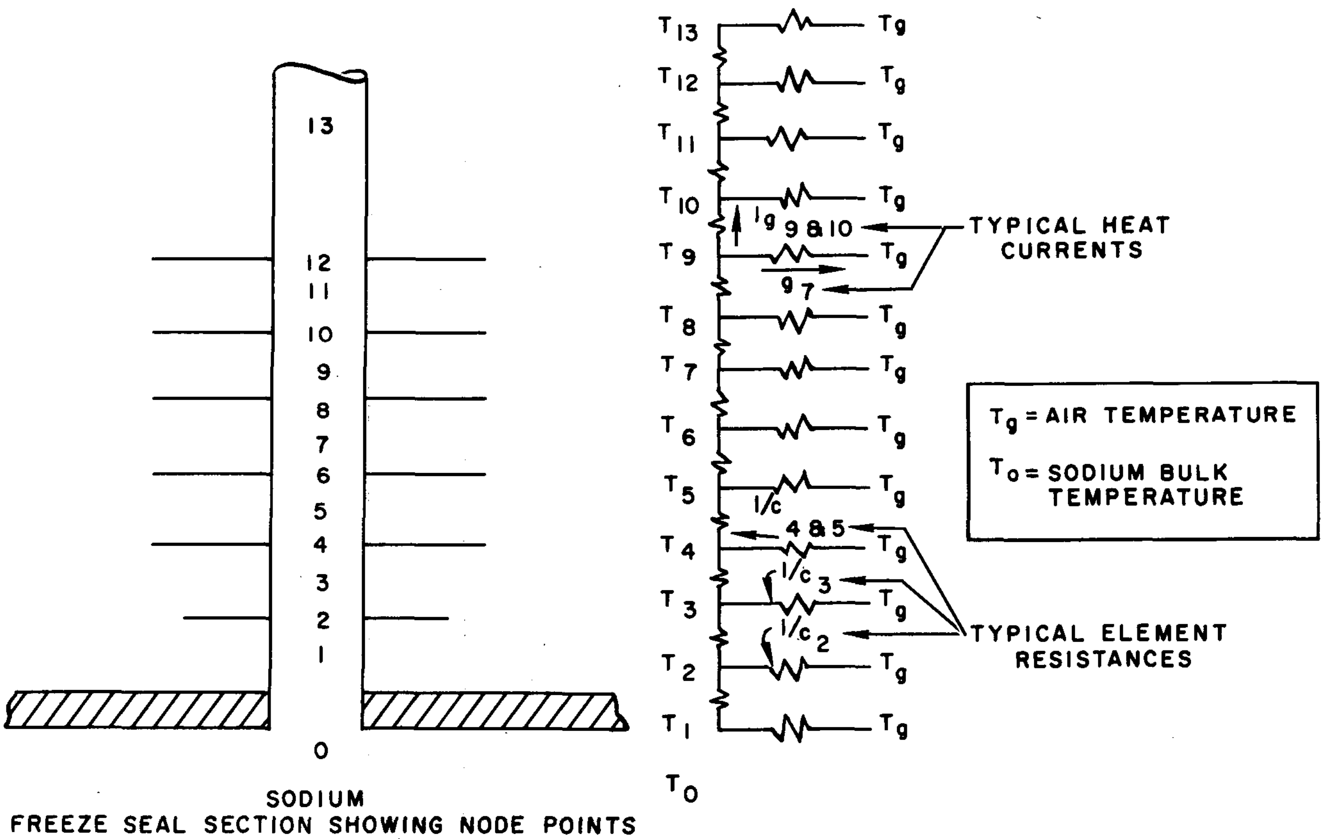

Figure 8. Method I Thermal Circuit

in this procedure that the horizontal stem cross sections normal to the stem axis are isotimic surfaces. An analysis is given in the Appendix which shows this to be an accurate assumption. The quantities of heat transferred in the various elements of the network are indicated by q, and the conductances of the various elements are denoted by c. The general calculation procedure is outlined below, and the meanings of all symbols are given in the nomenclature.

For heat transfer into the gas:

$$q_n = c_n \Delta T, \qquad \Delta T = T_n - T_g .$$

For heat conduction up the shaft:

$$q_{m-n} = c_{m-n} \Delta T, \qquad \Delta T = T_m - T_n .$$

Determining c_n

c_n, n odd, may be approximated as follows:

$$q_n = c_n \Delta T = 2\pi \ell_2 bk \sqrt{B} \left[\frac{I_1(\ell_2 \sqrt{B}) K_1(\ell_1 \sqrt{B}) - K_1(\ell_2 \sqrt{B}) I_1(\ell_1 \sqrt{B})}{I_1(\ell_2 \sqrt{B}) K_o(\ell_1 \sqrt{B}) + K_1(\ell_2 \sqrt{B}) I_o(\ell_1 \sqrt{B})} \right] \Delta T$$

$$= 2\pi \ell_1 bk \sqrt{B} \phi \Delta T$$

where

$$B = \frac{2h}{kb} .$$

Hence

$$c_n = 2\pi \ell_1 bk \sqrt{B} \phi$$

c_n, n even, may be approximated conservatively by taking

$$q_n \cong 2\pi \ell_1 U \Delta x \Delta T$$

where

$$U = \frac{1}{\frac{1}{h} + \frac{\ell_1}{k}}$$

therefore

$$c_n \cong 2\pi \ell_1 U \Delta x.$$

c_{m-n} may be determined as follows:

$$q_{m-n} = \frac{\Delta T}{\Delta x} \sum_{i=1}^{3} k_i A_i,$$

where i = 1, 2, 3 pertain to the stainless steel stem and body conduction paths and the sodium annular path, respectively. The term Δx refers to the distance between node points m-n.

Thus,

$$c_{m-n} = \frac{1}{\Delta x} \sum_{i=1}^{3} k_i A_i$$

The effective film coefficient used in calculating the conductances must consider both free convection and radiation cooling. For the thermal elements denoted by n odd, the free convection film coefficient was determined from the following relation[5]

$$h = 0.28\left(\frac{\Delta T}{d}\right)_d^{0.25}$$

For the elements of even n, the fins were treated as horizontal plates. The unit heat flux from a horizontal plate facing upward is given[6] by

$$q_u = 0.275(\Delta T)^{4/3},$$

and that from a horizontal plate facing downward is given by

$$q_d = 0.50 q_u.$$

In calculating the thermal conductance, an average convection film coefficient was used as given below

$$h = \frac{q_u + q_d}{\Delta T} = 0.21(\Delta T)^{1/3},$$

which holds for the turbulent range. (If the stem axis had been in a horizontal plane the following relations would have been used in determining the approximate film coefficient[7]:

$$\text{For} \quad 10^8 > (Gr \cdot Pr) > 10^4 \qquad Nu = 0.52\,(Gr \cdot Pr)^{1/4},$$

$$\text{For} \quad (Gr \cdot Pr) > 10^8 \qquad Nu = 0.126\,(Gr \cdot Pr)^{1/3}.$$

these expressions are for free convection about horizontal cylinders.) To the film coefficient for free convection was added that due to radiation[8] (in the case of the stem guide surfaces but not the circumferential fin elements).

$$h = \frac{0.173\,\epsilon_s\left[\left(\frac{T_{na}}{100}\right)^4 - \left(\frac{T_{ga}}{100}\right)^4\right]}{T_{na} - T_{ga}} .$$

It may be noted from Figures 4 and 5 that the results based on this method are somewhat in error. The transport of energy up the annulus by sodium free convection may account for the discrepancy between predicted and actual results. This effect is discussed further in a later section.

2. Method II

This method is based on the differential equation for heat transfer along a vertical relatively slender rod which extends into still gas from an insulated pot containing molten sodium. The general solution of the differential equation is

$$\Delta T = Me^{-\alpha x} + Ne^{\alpha x} \qquad \ldots (1)$$

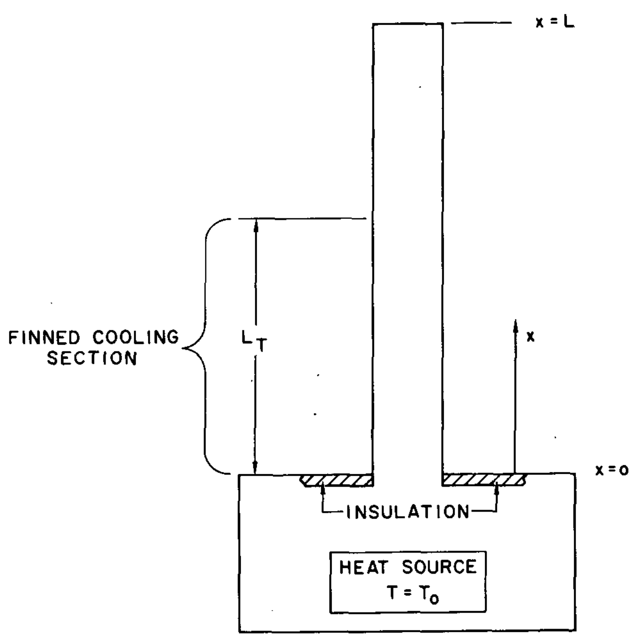

Figure 9. Idealized Heat Transfer Problem

where $\alpha = \sqrt{hD/kA}$ and x is the distance along the rod from the heat source as shown in Figure 9. The problem was treated in several different ways, each of which involved the use of different boundary conditions and consequent changes in the values of M and N. The numerical results for each of these treatments were, however, approximately the same so far as the cooling sections used in this experiment are concerned. Effective and average values were used for the terms in α. These will be discussed later. At this point the approaches to solution of the above differential equation will be briefly mentioned.

Considering the protruding shaft (stem, stem-guide, fins, etc.) to be a very long rod, the boundary conditions for Equation 1 are

$$\text{at } x = 0, \quad T = T_o,$$
$$\Delta T = \Delta T_o.$$

$$\text{and at } x = \infty \quad T = T_g,$$
$$\Delta T = 0 \qquad \ldots (2)$$

For these boundary conditions, the solution to Equation 1 is

$$\Delta T = \Delta T_o e^{-\alpha x} \qquad \ldots (3)$$

Taking the shaft to be of finite length with no heat loss from the end ($x = L$), the second boundary condition of Equation 2 is replaced by

$$\text{at } x = L, \quad \frac{d(\Delta T)}{dx} = 0 \qquad \ldots (4)$$

The solution of Equation 1 is then

$$\Delta T = \Delta T_o \frac{\cosh\left[(x-L)\alpha\right]}{\cosh(\alpha L)} . \qquad \ldots (5)$$

In the above relations, the effects of the stem guide sections with and without fins were lumped. The effects were separated by writing equations for each of the two sections as follows

$$\text{for } 0 < x < L_T \qquad \Delta T_1 = M_1 e^{-\alpha x} + N_1 e^{\alpha x}, \qquad \ldots (6)$$

for $L_T < x < L$, or $0 < y < L - L_T$, where $y = x - L_T$,

$$\Delta T_2 = M_2 e^{-\alpha' y} + N_2 e^{\alpha' y} \qquad \ldots (7)$$

where α' is the modulus that corresponds to the section without fins.

The boundary conditions for this case are

$$\text{at } x = 0, \; \Delta T_1 = \Delta T_o$$

$$\text{at } x = L_T, \quad y = 0, \quad \Delta T_1 = \Delta T_2$$

$$\frac{d(\Delta T_1)}{dx} = \frac{d(\Delta T_2)}{dy} \qquad \ldots (8)$$

$$\text{at } x = L, \quad y = L - L_T, \quad \frac{d(\Delta T_2)}{dy} = o$$

Obtaining the appropriate values for α and α' (these terms are discussed below) corresponding to the longitudinal fin arrangement for general conditions with $T_o = 1150°F$, Equations 6 and 7 become

$$\Delta T_1 = \Delta T_o e^{-4.40x}$$

$$\Delta T_2 = 0.0046 \Delta T_o e^{2.01y} + 0.0480 \Delta T_o e^{-2.01y} \qquad \ldots (9)$$

Similar relations were obtained for a bulk temperature of 1300°F. In the expression for $\alpha\left(=\sqrt{hD/kA}\right)$ an average value for the film coefficient (for radiation and convection) was assumed. After a temperature distribution was calculated, the assumed value was checked. The value of the product kA in the denominator was determined in the fashion described under Method I with the kA for the sodium being doubled (Figure 10), to provide a measure of allowance for convective effects. The value used for the perimeter D accounts for both the stem guide and

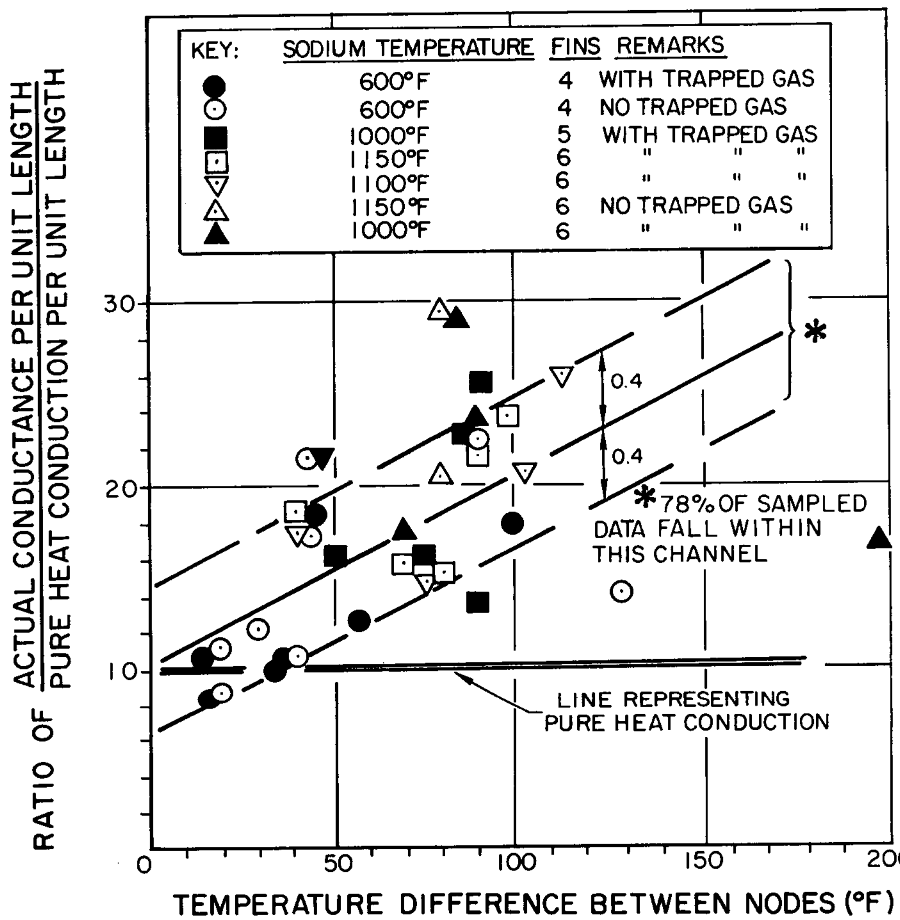

Figure 10. Effective Stem Conduction (based on experimental data selected at random)

the fins. The relation used was

$$D = S + \eta F, \qquad \ldots(10)$$

where S is the stem guide surface area per foot of length in contact with the surrounding atmosphere, and F is the fin surface area per foot of length. The fin effectiveness, η, is given by

$$\eta = \frac{\tanh w\sqrt{B}}{w\sqrt{B}} . \qquad \ldots(11)$$

As indicated previously, the several procedures described under Method II produced practically identical numerical predictions for the cases considered for this experiment. Examples of the predictions and actual results appear in Figures 4, 5, and 7. The agreement is good near the heat source, but as the stem temperature nears the freezing point of sodium there is a divergence between predicted and actual values. At the low temperatures the temperature vs distance curve slope is small, and, while in general the error in temperature magnitude might not be great, the predictions of distance from heat source to frozen sodium may be in significant error. For example, in Figure 7 the curve for $T_o = 1300°F$ shows a difference of approximately 3-in. between the predicted and actual location of the lowest level of frozen sodium in the seal. There is a marked improvement in the accuracy of predictions with reduction in T_o.

D. STEM CONDUCTANCE

Natural convection of sodium in the stem-stem guide annulus assisted in the transfer of energy up the stem. The total heat transferred was therefore greater than that which would have been transferred up the stem by conduction alone. An attempt was made to determine (on a gross basis) quantitatively the effect of this natural convection of sodium. The approach used involved the setup of a thermal network for the circumferential fin arrangement as described under Method I. The fin and stem perimeter conductances, c_n, were calculated. Knowing from the experiment the temperature corresponding to each node point, it was possible to calculate the heat currents, q_n. Then the heat transferred between stem node points, q_{m-n}, was determined by performing heat balances working backwards from the top end of the stem toward the heat source. Dividing the q_{m-n} by the ΔT_{m-n} gave the c_{m-n}. In Figure 10, several c_{m-n} values found from the experiment (to be referred to as "actual conductance") are compared with the c_{m-n} calculated for pure heat conduction on a unit length basis. The actual conductances are for experimental data sampled at random, and the comparison is based on temperatures between node points. A definite pattern evolved that showed that the actual conductance was twice that of pure heat conductance when the temperature difference between adjacent nodes was about 100°F. It will be recalled that the distance between adjacent rings was one inch. For greater distances between rings and for wider annuli (the annulus width was 11 mils) there may be a sizable increase in the conductance per unit length. In this connection, Reference 9 indicates that under certain conditions relatively large amounts of heat maybe transferred by free convection in sodium-filled annuli. A more refined analysis of the natural convection effects was not attempted because of the lack of highly accurate information on annulus temperatures and geometry.

E. STEM TORQUE, OXIDE EFFECTS

Measurements were made during the experiment of the torque required to rotate the stem. At the outset of the experiment, it was expected that increases in the torque measurements (for the same sodium conditions) could be interpreted as being caused by oxide buildup in the annulus. However, a slight misalignment caused by a modification (extension) of the stem guide resulted in rubbing of the stem against the stem guide near the top of the seal. This effect increased the amount of torque required to turn the stem and somewhat clouded comparisons between subsequent runs and the earlier runs.

With the experimental system dry, the torque-to-turn (to be referred to as V) was measured to be 30 in.-lb. When the system was full of sodium at temperatures between 600 and 1000°F, the V consistently appeared to be a function of pressure, varying between about 30 in.-lb for 1-5 psig sodium pressure and 60 in.-lb at 60 psig. The increase in V with sodium pressure was evidently due to the increase in bearing pressure between the ring and collar at the top of the stem. The stem-modification was accomplished after 336 hr of operation. There was undoubtedly oxygen contamination of the sodium at the top of the seal during the modification process. Immediately after the change, with sodium temperatures at 1150°F, the V values increased into the 100-250 in.-lb range. This increase was attributed to the presence of sodium oxide in the annulus. Later, during the first efforts to remove the gas trapped below the anticonvection rings, the sodium in the annulus was forced up into the gas chamber at the top of the seal. The extruded sodium (and sodium oxide) was carefully removed by hand from the gas chamber. Subsequently, when the unit returned to operation, the values measured for V were approximately the same (very slightly higher due to rubbing of stem on stem-guide) as those measured during the first experimental phase, before the 4-in. extension was added to the stem-guide. It was found that the torque required to initiate rotation of the stem could be accurately calculated using the known length of frozen sodium in the annulus and a solid sodium shear strength of 25 psi.

Based on the above evidence, it was concluded that no significant quantities of oxide diffused from the bulk sodium into the seal region. The initial oxide content in the sodium is estimated to have been 50 ppm, which would indicate a total system oxygen content of 1.5×10^{-3} lb of oxygen. It is possible that such a small quantity of oxygen would not have been detected, even though all oxide in the system concentrated in the cooling section.

IV. SUMMARY OF RESULTS

An experimental stem freeze-seal, suitable for a 6-in. valve size, operated satisfactorily under a variety of test conditions using two different cooling fin arrangements. Cooling of the seal region was accomplished by free convection to the ambient atmosphere. The operating conditions included sodium bulk temperatures up to 1300°F, sodium pressures up to 75 psig, and ambient temperatures as high as 150°F. Theoretically predicted and experimentally measured temperatures along the freeze seal were compared. Predictions were very accurate for a distance of several inches from the valve body, but in the lower temperature region of the seal the agreement is less favorable. It was noted that for a 1300°F sodium bulk temperature, the estimated length of frozen sodium, at the top of the seal, was almost 4-in. shorter than that established experimentally. Thus in this case the theoretical prediction produced conservative results. At lower bulk temperatures, the analytical predictions were more accurate. It was determined that one psig was the optimum constant gas backup pressure for the seal. There was no evidence of the diffusion of oxide from the sodium into the freeze seal region.

It is concluded that reliable and economical valve freeze seals for future high-temperature sodium systems may be designed based on the above results, i.e., using the implied corrections for analytical predictions.

APPENDIX

The purpose here is to examine the steady state temperature variation over a stem cross section normal to the stem vertical axis. The physical situation (at some distance from the valve body) is illustrated in Figure 11. This solid stem represents (for our purposes) a limiting case, since the actual experimental unit has a hollow stem. Since we are concerned only with effects in the radial direction, and because the temperature field is symmetrical about the axis, the terms involving the axial and angular coordinates are neglected. The determinative conditions are:

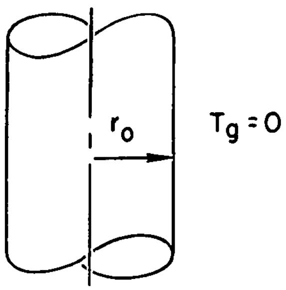

Figure 11.
Stem Section

$$T_g = 0 \qquad \ldots(1)$$

$$T = T(r) - T_g \qquad \ldots(2)$$

$$\frac{\partial T}{\partial r} = 0, \quad r = 0 \qquad \ldots(3)$$

$$-k\frac{\partial T}{\partial r} = hT, \quad r = r_o \qquad \ldots(4)$$

Using r_o as a unit length (and adjusting the values of physical constants accordingly), and substituting $h_g = \frac{h}{k}$, the last condition becomes

$$\frac{\partial T}{\partial r} + h_g T = 0, \quad r = 1. \qquad \ldots(5)$$

The continuity equation in polar coordinates for steady state is

$$\frac{1}{r}\frac{d}{dr}\left(r\frac{dT}{dr}\right) = 0 \qquad \ldots(6)$$

The Hankel transform of the temperature is defined[10] as

$$\overline{T}(p) = \int_o^1 T(r) r J_n(pr)\, dr. \qquad \ldots (7)$$

Integrating Equation 6 in accordance with Equation 7 and using Equation 5 gives

$$\int_o^1 \frac{d}{dr}\left(r\frac{\partial t}{\partial r}\right) J_o(pr)\, dr = J_o(p)\left[\frac{\partial T(1)}{\partial r} + h_g T(1)\right] - p^2\overline{T},$$

where the terms within the brackets will be carried for reasons to become apparent shortly. The transformed temperature is then

$$\overline{T} = \frac{J_o(p)\left[\frac{\partial T(1)}{\partial r} + hgT(1)\right]}{p^2}, \qquad \ldots (8)$$

and when Equation 8 is substituted into the following inversion expression[11]

$$T(r) = 2\sum_p \frac{p^2\overline{T}}{h_g^2 + p^2} \frac{J_o(pr)}{J_o^2(p)}, \qquad \ldots (9)$$

the result is

$$T(r) = 2\sum_p \frac{J_o(pr)}{J_o(p)\left(h_g^2 + p^2\right)}\left[\frac{\partial T(1)}{\partial r} + h_g T(1)\right], \qquad \ldots (10)$$

where the p are roots of

$$p\,J_o^{1}(p) + h_g J_o(p) = -pJ_1(p) + h_g J_o(p) = 0 \qquad \ldots(11)$$

Evaluating Equation 10 at r = 1 gives

$$T(1) = 2\left[\frac{\partial T(1)}{\partial r} + h_g T(1)\right]\sum_p \frac{1}{\left(h_g^{\,2} + p^2\right)},$$

which solving for T(1), gives

$$T(1) = 2\,\frac{\partial T(1)}{\partial r}\,\frac{\displaystyle\sum_p \frac{1}{h_g^{\,2} + p^2}}{1-2h_g\displaystyle\sum_p \frac{1}{h_g^{\,2} + p^2}} \qquad \ldots(12)$$

Evaluating Equation 10 at r = 0 gives

$$T(o) = 2\left[\frac{\partial T(1)}{\partial r} + h_g T(1)\right]\sum_p \frac{J_o(o)}{J_o(p)\left(h_g^{\,2} + p^2\right)} \qquad \ldots(13)$$

Substituting T Equation 1 from Equation 12 in Equation 13 and solving for $\frac{\partial T(1)}{\partial r}$ gives

$$\frac{\partial T(1)}{\partial r} = T_o\,\frac{\left[1 - 2\,h_g\displaystyle\sum_p \frac{1}{h_g^{\,2} + p^2}\right]}{\left[2\displaystyle\sum_p \frac{1}{J_o(p)\left(h_g^{\,2} + p^2\right)}\right]} \qquad \ldots(14)$$

The roots of Equation 11 were found by a graphical method to be $p \cong 0$, $p = 3.85$, 7.02, 10.17, 13.32... The value of h_g based on r_o is approximately 0.003/unit length.

The series embodied in Equation 14 converge rapidly with the result

$$\frac{\partial T(1)}{\partial r} \cong - h_g T_o . \qquad \ldots(15)$$

Comparing this result with Equation 5 shows that

$$T(1) \cong T(o), \qquad \ldots(16)$$

and the agreement is better than within 0.1%. The chief reason for this is the effect of the very small h_g (due to the small h for free convection in air), which has an insulating influence at the stem surface.

NOMENCLATURE

A = area, ft^2
b = fin thickness, ft
B = $2\ h/kb$
c = overall conductance term, Btu/hr°F
C_p = specific heat, Btu/lb°F
d = distance between circumferential fins, ft
D = perimeter, ft^2/ft
F = area of fin surfaces in contact with air, ft^2/ft
Gr = Grashof modulus, $H^3 \beta g \Delta T/\nu^2$
g = acceleration due to gravity, ft/hr^2
H = characteristic length, ft
h = heat transfer coefficient Btu/hr°F ft^2
I_n = modified Bessel function of first kind, order n
J_n = Bessel function of first kind, n order
K_n = Modified Bessel function of second kind, n order
k = thermal conductivity
ℓ_1 = outside radius of stem guide, ft
ℓ_2 = outside radius of circumferential fin, ft
L = total shaft length, ft
L_T = length of finned section, ft
M, M_1, M_2 = constants of integration
N, N_1, N_2 = constants of integration
Nu = Nusselt modulus, hH/k
p = transform variable
Pr = Prandtl modulus, $\frac{C_p \mu}{k}$
q = heat flux, Btu/hr
q_d = unit heat flux from plate facing down, Btu/hr ft^2
q_u = unit heat flux from plate facing upwards, Btu/hr ft^2
r = radial coordinate, ft
S = area of stem guide surface in contact with atmosphere, ft^2/ft
ΔT = temperature difference, °F
$\overline{T}$ = Hankel transform of temperature
T_g = gas temperature, °F
T_n = temperature at node point n, °F
T_o = sodium bulk temperature, °F
U = overall heat transfer coefficient, Btu/hr °F ft^2
V = torque to rotate stem, in.-lbs
w = fin width, ft
Δx = distance between node points, ft
x = distance along shaft from heat source, ft
y = $x - L_T$, for $x > L_T$
α, α' = $\sqrt{hD/kA}$
β = coefficient of thermal bulk expansion, 1/°F
ϵ_s = emissivity (taken to be equal to absorptivity)
η = fin efficiency
ϕ = function in circumferential fin conductance term
μ = dynamic viscosity, lb/ft hr
ν = kinematic viscosity, ft^2/hr

Subscripts

m, n = relate to node point
a = absolute temperature, °R

REFERENCES

1. Liquid Metals Handbook, AEC-USN pub. TID 5277, Sodium-NaK Supplement, 1955
2. W. B. Cottrell, and L. A. Mann, ORNL-1688, 1953
3. Unpublished work by R. Cygan
4. K. A. Tomblin, et al., AERE ED/M.9, March 1954
5. M. Jakob, Heat Transfer, Wiley and Sons, New York, Vol. I, 1949, p 529
6. Ibid, p 532
7. Ibid, p 525
8. W. H. McAdams, Heat Transmission, (3rd Ed., McGraw-Hill, New York, 1954) p 63
9. D. P. Timo, KAPL-M-DPT-8, 1955
10. C. J. Tranter, Integral Transforms in Mathematical Physics, (Wiley and Sons, New York, 1954) p 2
11. Ibid, p 88